Supporting Information

Deep Surface Passivation for Efficient and Hydrophobic Perovskite Solar Cells

Junmin Xia, [a, 1] *Chao Liang,* [a, 1] *Shiliang Mei,* [a] *Hao Gu,* [a] *Bingchen He,* [a] *Zhipeng Zhang,* [a] *Tanghao Liu,* [a] *Kaiyang Wang,* [a] *Sisi Wang,* [a] *Shi Chen,* [a] *Yongqing Cai* [a, *] *and Guichuan Xing* [a, *]

[a] Joint Key Laboratory of the Ministry of Education, Institute of Applied Physics and Materials Engineering, University of Macau, Avenida da Universidade, Taipa, Macau 999078, P. R. China

Corresponding Author

*E-mail: gcxing@um.edu.mo (G. Xing), E-mail: yongqingcai@um.edu.mo (Y. Cai)

[1] J. Xia and C. Liang contributed equally to this work.

Note S1: Space-charge-limited-current (SCLC) technique.

The trap densities (N_t) in perovskite films were figure out by the space-charge-limited-current (SCLC) technique.[1] An electron-only device with a glass/ITO/SnO_2/perovskite/PCBM/Ag architecture (Fig. S2a) and a glass/ITO/PEDOT:PSS/perovskite/spiro-OMeTAD/Ag hole-only device (Fig. S2c) were fabricated. Fig. S2b illustrates the dark current-voltage (J-V) characteristics of the pristine and CF_3PEAI 2D passivated electron-only devices, which shows a linear ohmic region, a trap-filling limited region, and a trap-free child's region. The electron trap density can be calculated with trap-filled limit voltage (V_{TFL}) from the following equation:

$$N_t = \frac{2V_{TFL}\varepsilon_r\varepsilon_0}{qL^2} \quad (1)$$

Where ε_r is the relative dielectric constant of perovskite (ε_r = 32),[2] ε_0 is the vacuum permittivity, V_{TFL} is the onset voltage of the trap-filled limit region, q is the elemental charge, and L is the thickness of the perovskite film (~ 800 nm). The electron trap density in the 2D passivated perovskite is figured out to be 2.25×10^{15} cm^{-3}, which is much lower than the pristine (4.5×10^{15} cm^{-3}) perovskite. Similarly, a hole trap density of 3.75×10^{15} cm^{-3} and 2.68×10^{15} cm^{-3} are achieved for the pristine and 2D CF_3PEAI passivated films (Fig. S2d). The reduced trap state density in the passivated film could be attributed to the high-quality perovskite crystals. It can improve performance and mitigate the hysteresis effect in PSCs.

Experiment section

Materials: The SnO_2 colloid precursor was purchased from Alfa Aesar. N, N-dimethylformamide (DMF), isopropanol (IPA), and dimethyl sulfoxide (DMSO) were purchased from Sigma-Aldrich. PbI_2, formamidine iodide (FAI), methylamine hydrobromide (MABr), methylammonium chloride (MACl), PEAI, CF_3PEAI, and Spiro-OMeTAD were purchased from Xian Polymer Light Technology Corp. All materials were used without any further purification.

Fabrication of PSCs: The ITO glasses were ultrasonically cleaned with deionized water, acetone, and isopropanol for 10 minutes, respectively. Then the clean glasses were dried in the drying oven and then treated with UV-ozone for 10 min. The SnO_2 colloid precursor was diluted with deionized water in a volume ratio of 1: 6. The electron transport layer (ETL) layer was prepared by spin coating the SnO_2 precursor at 3,000 rpm for 40 s and then annealed at 150 ^oC for 30 min. Before transferred into the glovebox, the substrates were treated with the UV-ozone again. For the perovskite layers, a two-step process was employed. Firstly, PbI_2 (654 mg) was dissolved in a mixed solvent of DMF and DMSO (1 mL, volume ratio at 4:1). After complete dissolution, the PbI_2 solution was filtered through a 0.22 μm pore polytetrafluoroethylene filter and then was spin-coated onto the HTL layers at 1,600 rpm for 20 s and 4,000 rpm for 30 s successively. After then, the PbI_2 film was annealed at 72 ^oC for 2 min. Later, the mixed cations isopropanol solution (220 mg FAI, 22 mg MABr, and 23 mg MACl dissolved in 1,500 μL isopropanol) was spin-coated onto the PbI_2 layer at 2,000 rpm for 30 s. Then the perovskite films were annealed at 150 ^oC for 30 min in the ambient environment (40% relative humidity). For the passivation treatment, CF_3PEAI solutions in isopropanol with different concentrations (1, 2, 5, and 10 mg/mL) were spin-coated onto perovskite films at 4,000 rpm for 30 s, and then the films were annealed at 100 ^oC for 10 min to form the 2D perovskite. The HTL was then deposited by spin coating at 3,000 rpm for 30 s, and it contains Spiro-OMeTAD (72.3 mg), bis(trifluoromethane) sulfonamide lithium salt (Li-TFSI) stock solution (17.5 μL, 520 mg Li-TFSI in 1 mL acetonitrile), 28.8 μL 4-tertbutylpyridine in the 1 mL chlorobenzene. At last, after being oxidized for 24 h in the desiccator, 80 nm Au film was thermal evaporated as the electrode.

Characterization: The XRD patterns information was characterized by a Rigaku (RINT-2500) X-ray diffractometer (Cu Ka radiation, λ=1.5418 A), operating at 45 kV and 200 mA over the angular range $10° \leq 2\theta \leq 90°$. UV–vis–NIR fluorescence spectrophotometer absorption spectra were performed by a Shimadzu UV 3600 spectrophotometer at room temperature. Morphologies images were depicted by a field emission scanning electron microscope (JEM-7500F). XPS measurements were carried out with a PHI Quantum 2000 device (Physical Electronics, USA), using a monochromatic Mg Kα source and a charge neutralizer. All the binding energies were revised according to the C 1s peak of the surface adventitious carbon at 284.6 eV. AFM images were tested by a Dimension Fastscan Atomic Force Microscope (Bruker Fastscan). PL (excitation at 450 nm) was performed with the Hamamatso spectrometer. The J-V curves characteristics were tested with a Keithley 2420 source meter and 425W collimated Xenon lamp (Newport). A PHI5000 Versa Probe instrument collected the UPS parameters. The UPS radiation was raised by a He-gas discharge lamp (He Iα at 21.22 eV). The TCSPC was performed at room temperature. The excitation source was a pulsed ultraviolet picosecond diode laser operating at 405 nm. The signal was dispersed by a 320 mm monochromator (iHR320 from Horiba, Ltd.) combined with suitable filters and detected based on the time-correlated single photon counting technique.

Computational details: DFT calculations are performed using the Vienna Ab Initio Simulation Packages (VASP) with the spin-polarized generalized gradient approximation (GGA) proposed by Perdew–Burke–Ernzerhof (PBE).[3] The structure relaxations are carried out with a 400 eV plane-wave cutoff, and the van der Waals force correction is considered with the DFT-D3 method of Grimme.[4] The Brillouin Zone integration was sampled following a gamma-centered Monkhorst-pack scheme,[5]

using 1 × 1 × 1 k-point grids for the ionic optimization and 3 ×3 ×3 for the density of state, respectively. The self-consistent total-energy difference and the convergence criterion for forces on atoms are set to 10^{-4} eV and 0.01 eV/Å, respectively. In all the calculations, the first two layers on the $FAPbI_3$ slab surface under investigation are fully relaxed, while the positions of other layers at the bottom are kept fixed. A vacuum spacing > 15 Å is used to prevent inter-slab interactions.

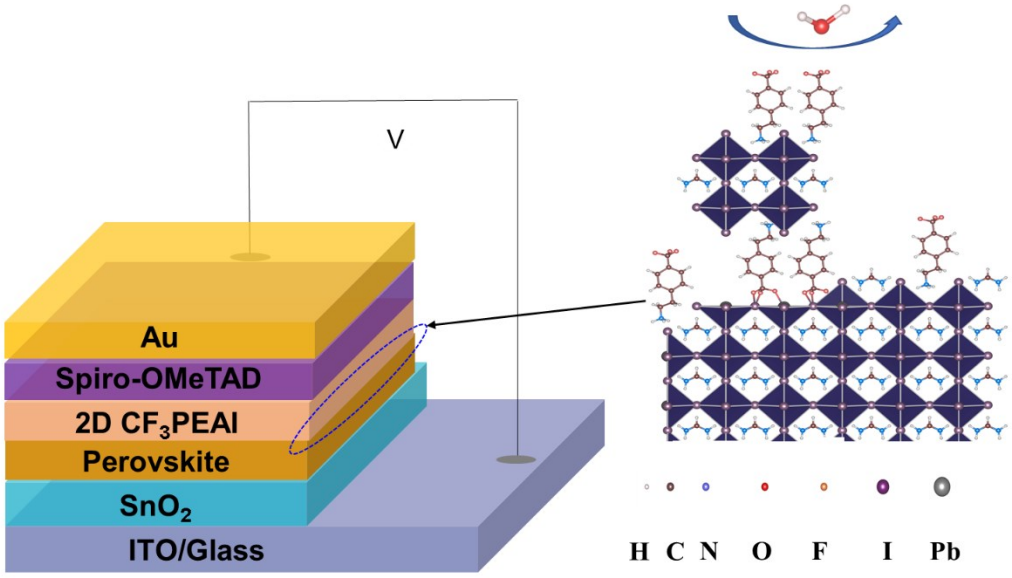

Fig. S1. Structure of the devices applied in the study and the proposed mechanism of CF_3PEAI passivating the perovskite layer.

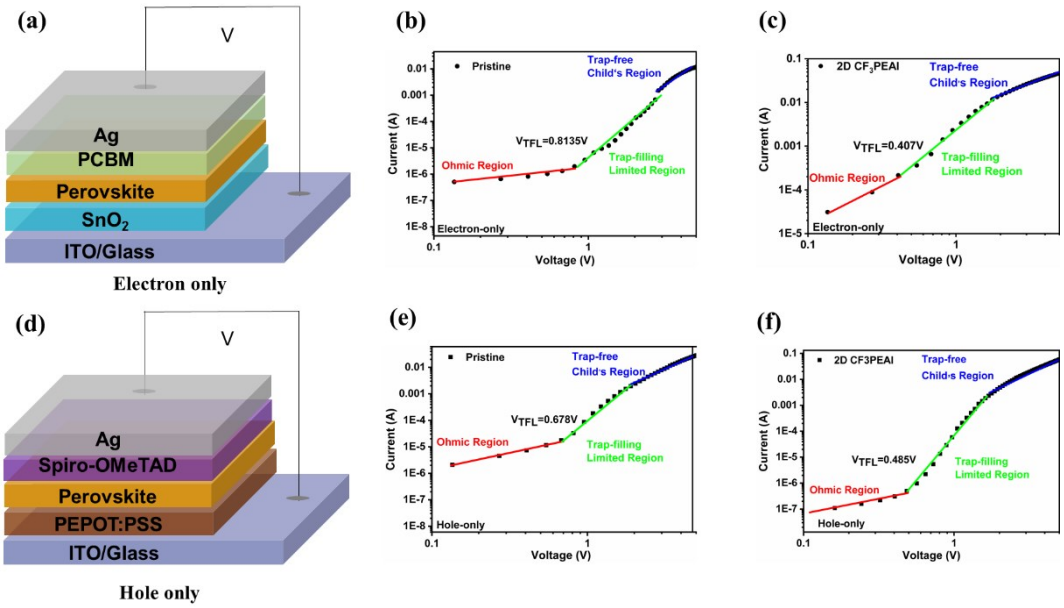

Fig. S2. Current-voltage measurement of the electron-only and hole-only devices. Structure of electron-only devices (a); Dark current-voltage curve for the electron-only device of the pristine (b) and CF_3PEAI 2D passivated (c); Structure of hole-only devices (d); Dark current-voltage curve for the hole-only device of the pristine (e) and CF_3PEAI 2D passivated (f).

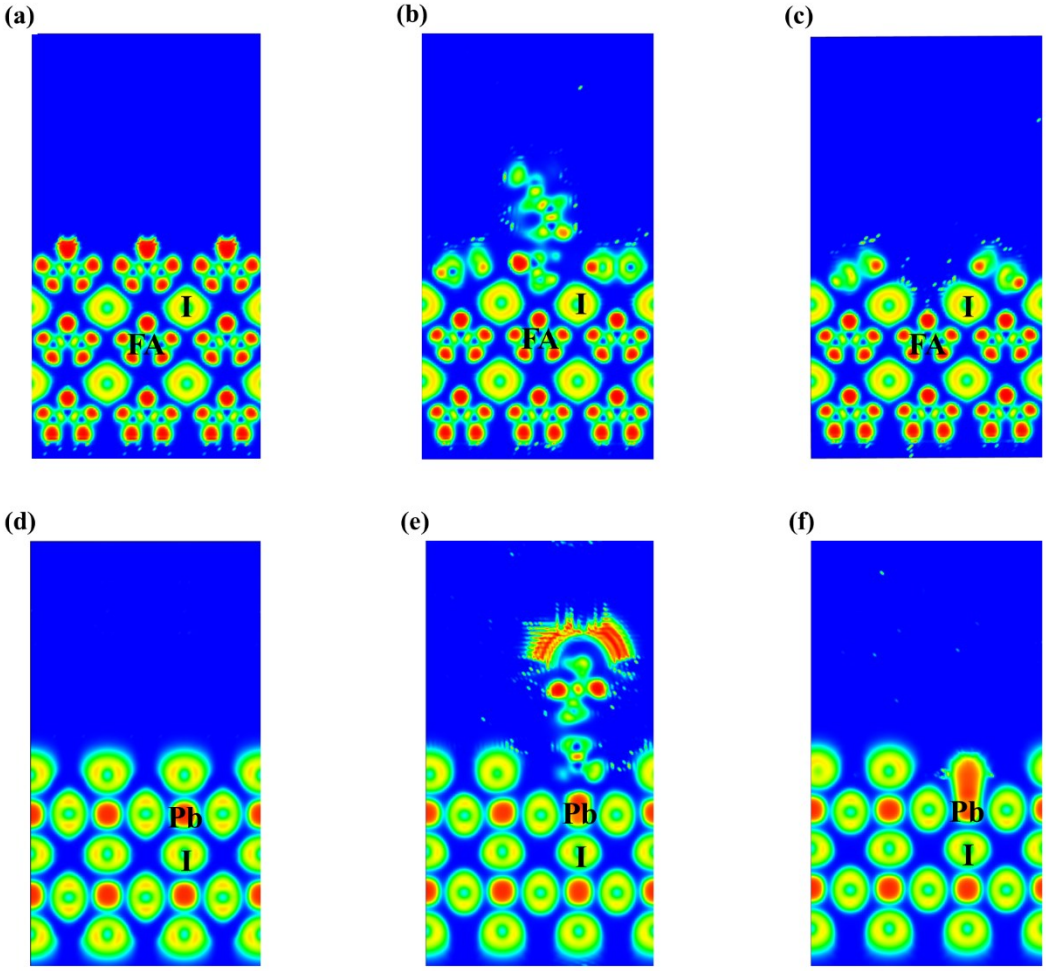

Fig. S3. Electron localization function results of $FAPbI_3$ for FA vacancy (a) perfect; (b) passivated and (c) with V_{FA}; Electron localization function results of $FAPbI_3$ for I vacancy (d) perfect, (e) passivated, and (f) withV_I.

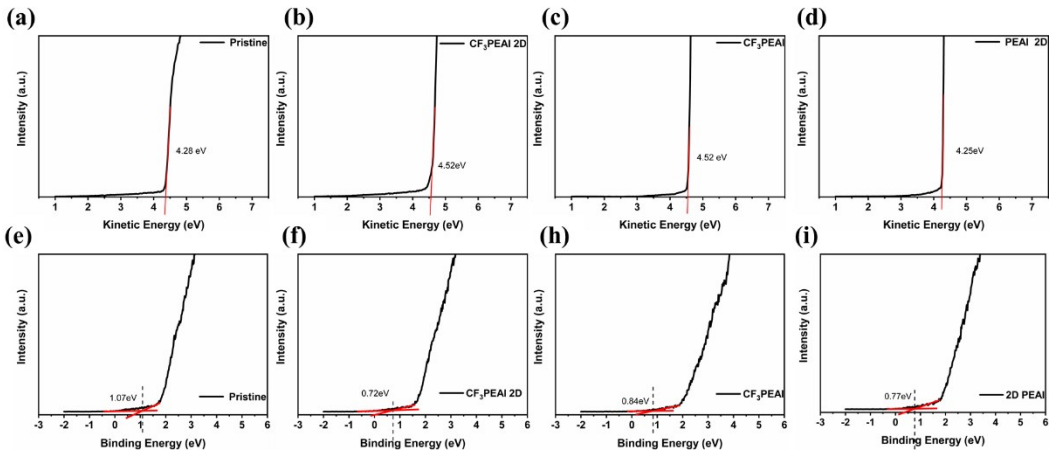

Fig. S4. Ultraviolet photoelectron spectroscopy (UPS). Helium Iα (hν = 21.22 eV) spectra of work function (a) the pristine; (b) CF_3PEAI 2D passivated; (c) CF_3PEAI passivated; (d) PEAI 2D passivated; and VBM with respect to the Fermi level (e) the pristine; (f) CF_3PEAI 2D passivated; (g) CF_3PEAI passivated and (h) PEAI 2D passivated.

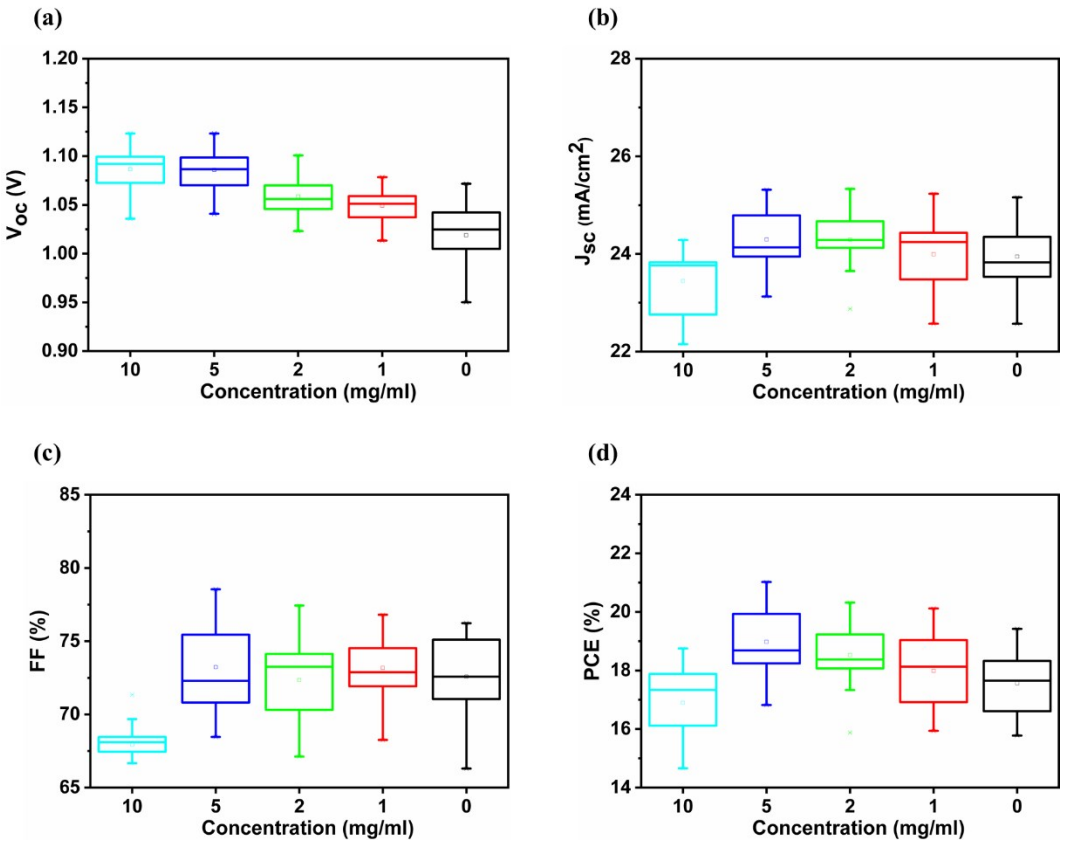

Fig. S5. Statistical data for (a) V_{OC}, (b)J_{SC}, (c) FF, and (d) PCE obtained from 20 cells per condition with different concentrations CF_3PEAI 2D passivated.

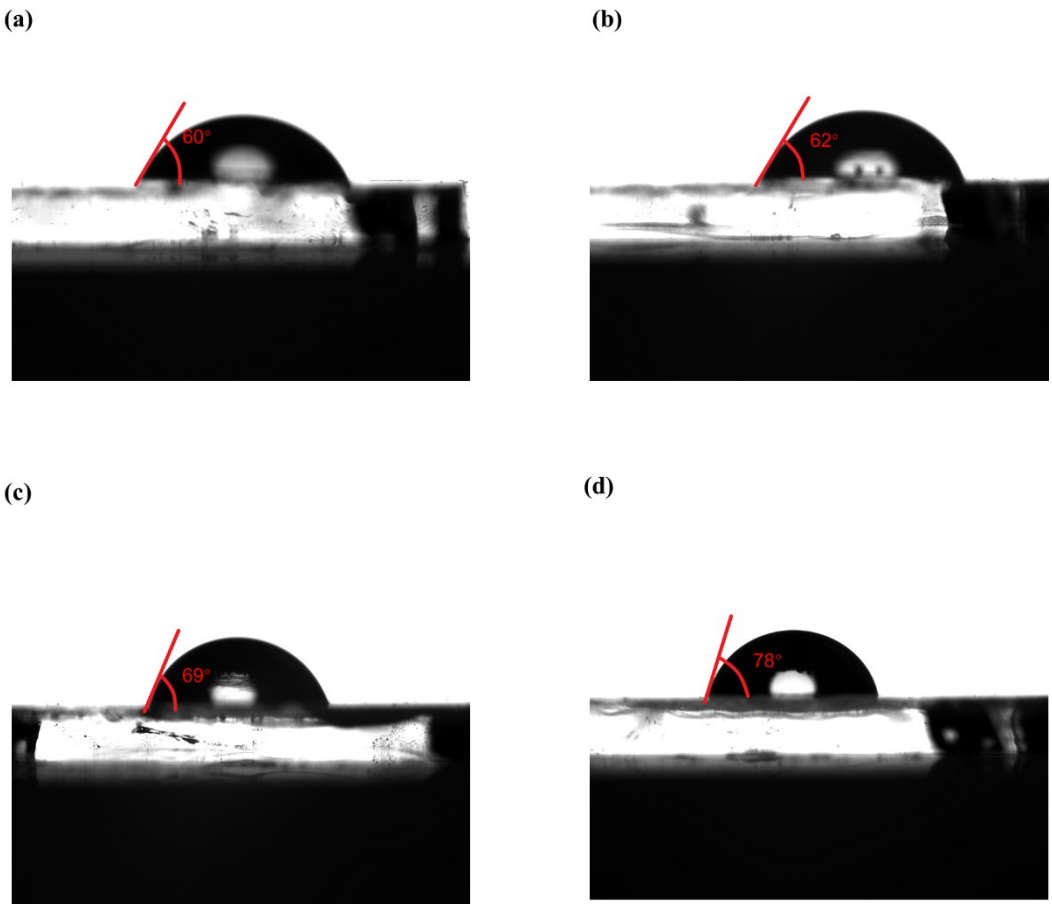

Fig. S6. The contact angle with deionized water of the films: (a) The pristine; (b) The PEAI 2D passivated; (c) The CF_3PEAI passivated; (d) The CF_3PEAI 2D passivated.

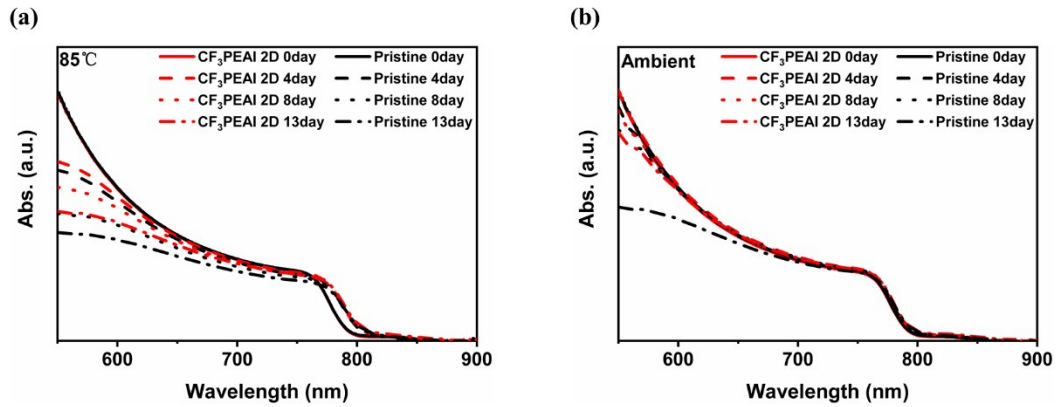

Fig. S7. UV–Vis absorbance spectra evolution of the perovskite films at 85 ℃ in the nitrogen glove box (a), and in ambient (RH, 70-80%) (b).

Table S1. The time coefficients and relative magnitude of PL decay trace in Fig. 1d.

	τ_1 (ns)	A_1 (%)	τ_2 (ns)	A_2 (%)	τ_{av} [a] (ns)
Pristine	110.10	12.76	511.68	87.24	460.42
CF_3PEAI 2D	105.29	1.17	1674.67	98.83	1656.30
CF_3PEAI	110.05	3.02	746.43	96.98	727.20
PEAI 2D	77.02	5.63	1575.41	94.37	1491.05

[a] τ_{av} is the Amplitude-weighted average lifetimes;

Table S2. Summary performance of devices (0.05 cm^2 aperture) with different surface treatment under simulated AM 1.5G solar irradiation at 100 mW cm^{-2}. The devices were measured from reverse scans (from 1.2 V to 0 V).

	V_{OC} (V)	J_{SC} (mA/cm^2)	Fill Factor (%)	PCE (%)
Pristine	1.04	24.08	74.78	18.87
CF_3PEAI 2D	1.11	24.25	78.21	21.05
CF_3PEAI	1.08	24.02	75.55	20.28
PEAI 2D	1.09	23.61	78.04	20.12

Table S3. Performance of the CF_3PEAI 2D treated devices and the pristine (0.05 cm^2 aperture). Here, H-index define as: H-index= $(PCE_{reverse} - PCE_{forward})/PCE_{reverse}$.

Samples	Scan Direction	V_{OC} (V)	J_{SC} (mA/cm^2)	Fill Factor (%)	PCE (%)	H-index
Passivated	Forward	1.09	24.04	78.44	20.55	2.38%
	Reverse	1.11	24.25	78.21	21.05	
Pristine	Forward	1.01	24.01	71.27	17.31	8.27%
	Reverse	1.04	24.08	74.78	18.87	

Reference

[1] D. Luo, W. Yang, Z. Wang, A. Sadhanala, Q. Hu, R. Su, R. Shivanna, G.F. Trindade, J.F. Watts, Z. Xu, T. Liu, K. Chen, F. Ye, P. Wu, L. Zhao, J. Wu, Y. Tu, Y. Zhang, X. Yang, W. Zhang, R.H. Friend, Q. Gong, H.J. Snaith, R. Zhu, *Science* **2018**, 360, 1442-1446.

[2] Q. Dong, Y. Fang, Y. Shao, P. Mulligan, J. Qiu, L. Cao, J. Huang, *Science* **2015**, 347, 967-970.

[3] J.P. Perdew, K. Burke, M. Ernzerhof, *Phys. Rev. Lett.* **1996**, 77, 3865-3868.

[4] G. Kresse, D. Joubert, *Phys. Rev. B* **1999**, 59, 1758-1775.

[5] H.J. Monkhorst, J.D. Pack, *Phys. Rev. B* **1976**, 13, 5188.